



## Effect of operating parameters on temperature and concentration polarization in vacuum membrane distillation process

Eunkyung Jang<sup>a</sup>, Sook-Hyun Nam<sup>b</sup>, Tae-Mun Hwang<sup>a,b,\*</sup>, Sangho Lee<sup>c</sup>, Yongjun Choi<sup>d</sup>

<sup>a</sup>School of Environmental Engineering, University of Science & Technology, 217 Gajungro Yuseong-gu, Daejeon 305-333, Korea, Tel. +82 31 910 0741; Fax: +82 31 910 0291; email: [taemun@kict.re.kr](mailto:taemun@kict.re.kr) (T.-M. Hwang)

<sup>b</sup>Korea Institute of Construction Technology, 2311 Daehwa-Dong, Ilsanseo-Gu, Goyang-Si, Gyeonggi-Do 411-712, Korea

<sup>c</sup>School of Civil and Environmental Engineering, Kookmin University, 861-1 Jeongneung-dong, Seongbuk-gu, Seoul 136-702, Republic of Korea

<sup>d</sup>Civil Engineering Department, Kyungnam University, Masan 631-701, Republic of Korea

Received 28 January 2014; Accepted 4 August 2014

---

### ABSTRACT

Membrane distillation is a process combining thermal and membrane technology, which uses the vapor pressure difference as driving force because of the temperature difference. Of the MD configurations, VMD can achieve high flux due to the application of vacuum. This paper analyzes operating parameters (vacuum pressure, feed flow rate, and feed concentration) that affect permeate flux in a modified design VMD system vacuum multi-effect membrane distillation (V-MEMD). The study investigated the most suitable operating parameters that would enhance the performance of V-MEMD system at high salinity (1–4 M of NaCl) with a moderate bulk temperature of 60°C. The result of this study showed that vacuum pressure is the most influential factor of the selected, and the effect of temperature polarization is more dominant to permeate flux than concentration polarization. Above this, the high-salinity solution can be treated by V-MEMD system because it does not affect the permeate total dissolved solid and flux. A dominant reduction ratio of vapor pressure was observed even at a low ratio of temperature polarization.

*Keywords:* Concentration polarization; Temperature polarization; Vacuum membrane distillation

---

### 1. Introduction

Membrane distillation (MD) is a process combining thermal and membrane technology. The main driving force in MD is the vapor pressure gradient created by the temperature difference across a hydrophobic

membrane [1]. Hence, increasing the vapor pressure gradient would result in higher permeate flux [2]. MD consumes less thermal energy due to lower temperature range between 20 and 80°C in comparison to conventional thermal distillation. As such, MD can operate with alternative energy, such as waste heat and solar energy, which reduces the consumption of fossil fuel requirement. Further, a salt rejection could

---

\*Corresponding author.

Presented at the 6th International Conference on the "Challenges in Environmental Science and Engineering" (CESE-2013), 29 October–2 November 2013, Daegu, Korea

be reached almost 100%, producing high-quality distillate [3]. In terms of configuration, the four commercially known MD configurations are direct-contact membrane distillation (DCMD), air-gap membrane distillation, sweeping gas membrane distillation, and vacuum membrane distillation (VMD). Among them, VMD is able to obtain higher flux due to the incorporation of vacuum pressure at the permeate side. The presence of vacuum reduces mass transfer resistance and heat loss through the membrane. A number of research papers have been published with regard to MD for various feed solutions including seawater, humic acid, sodium chloride (NaCl), and volatile substance [3]. However, the experimental studies were mostly using small-scale devices. Recently, Memsys produced a modified VMD configuration which is referred to as vacuum multi-effect membrane distillation (V-MEMD). Due to the modified design, the V-MEMD system has been reported to be able to obtain a high recovery rate of around 70–80% [4].

The permeate flux in the VMD process is impacted by factors such as feed concentration, temperature, flow rate, and vacuum pressure, as well as the membrane properties [5]. A number of previous studies have pointed out that feed temperature is one of the most influencing operating parameters to increase permeate flux. However, many of these studies have also acknowledged that high feed temperature results in higher temperature polarization effect and required more thermal energy [6–8]. The aim of this study was to investigate the most suitable operating parameters that would enhance the performance of V-MEMD system at high salinity (1–4 M of NaCl) with a moderate steam raiser temperature of 60°C. The investigation

also analyzed the impact of the selected operating parameters on the temperature polarization and concentration polarization through a model suitable for the device. Additionally, the contribution of polarization to the permeate flux was also determined by the model.

## 2. Material and methods

### 2.1. V-MEMD and operating conditions

The V-MEMD system concept is a combination of vacuum MD process and multistage flash distillation process. The multi-effect refers to the effect of heating, evaporation–condensation as well as condensing. In this system, heating effect and condensing effect take place internally through the steam raiser module and the condensing module, respectively. That apart, it is possible to incorporate multiple membrane stages into a V-MEMD system for the evaporation–condensation effect. By consecutively combing a number of membrane stages, there is an advantage of being able to continuously use the latent heat of vapor generated in the previous membrane stage also in the next stage. Moreover, because feed solutions go through a number of membrane stages, a high recovery rate can be obtained compared with other systems.

Fig. 1 presents a single membrane stage V-MEMD system used in this study. As shown in Fig. 2, V-MEMD module is classified into steam raiser (heating effect); effect stage (evaporation–condensation effect), where evaporation and condensation is generated simultaneously; and condenser (condensing

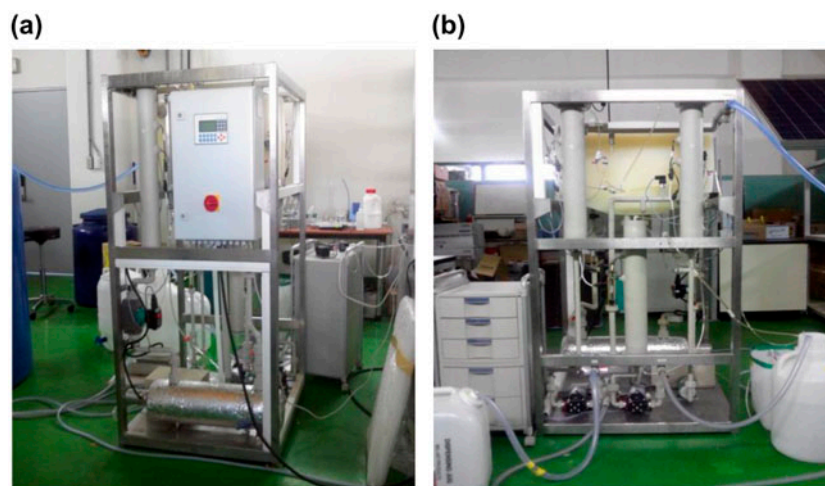


Fig. 1. Memsys V-MEMD system: (a) front and (b) back.

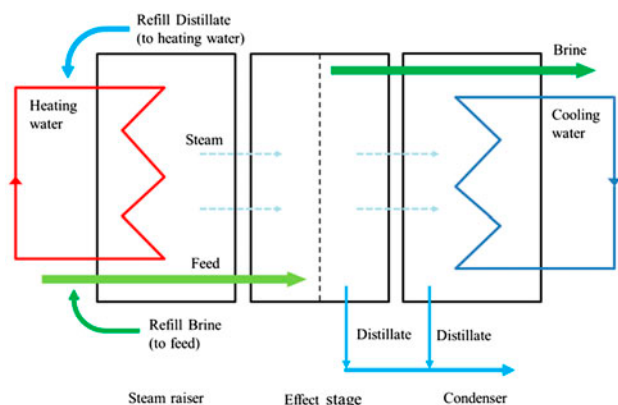


Fig. 2. Schematic diagram of the water flow on Memsys V-MEMD system.

effect). In the steam raiser, DI water is heated up internally and this generates steam (evaporation effect). The membrane stage consists of condensing foil, feed channel, and a flat sheet membrane. The foil performs the role of condensing the steam that generated from the steam raiser. Heat released from condensing steam is used to increase the feed solution temperature. The hydrophobic membrane that is fixed on the frame made by plastic allows only vapor to pass through it (evaporation–condensation effect).[9] The vapor that has passed through the hydrophobic membrane comes in contact with the condenser. And then, it is condensed and discharged out of the system (condensing effect). The condenser has continuous water flow to maintain a temperature of 25°C. The membrane used in this study is GE's PTFE membrane with an area of 0.16 m<sup>2</sup>, thickness of 20 μm, pore size of 0.2 μm, and porosity of 70–75%.

Aqueous solution of 1 M NaCl was used for the feed solution, and it was operated as batch type until it was concentrated from 1 to 4 M. Sigma–Aldrich reagent (purity 99.8%, NaCl) was used in solute for the feed solution. An initial feed solution of 10 kg was used in this experiment. Flux was calculated by the weight of the produced water (distillate) that is measured by 1 min interval. A CAS's CBX22KH balance was used for measuring the distillate weight and this data were sent to a computer using OHAUS's program (program name: Balance Talk). The permeate flux was calculated using weight difference according to the time of the produced water. In addition, the concentration of the total dissolved solid (TDS) of the produced water was measured by Thermo Scientific's Orion 3 Star conductivity portable.

To investigate the effect of operating parameters, such as (i) vacuum pressure, (ii) feed flow rate, and

(iii) feed concentration, four sets of operating conditions were chosen as shown in Table 1. For all the set of experiments, steam raiser temperature was set at 60°C. The initial feed concentration was 1 M of NaCl and it was concentrated to 4 M due to recirculation of brine to feed tank during filtration.

## 2.2. Modeling

### 2.2.1. Calculation of permeate flux

The device used in this research has a difference with previous researches [8,10]. In this study, actual size module that consisted of flat sheet membrane was used, not a cell unit mainly used in a lab-scale device. Moreover, the modeling was carried out using a theoretical equation of the MD technology that is selected considering that it is suitable for the device configuration and principle, and conducted comparative analysis with experimental values. The modeling of a module scale is a step required to scale up the lab-scale device and can be used in evaluating and optimizing the performance of the device. The basic equation of the MD technology was described as the following. The permeate flux of the MD system was calculated using Eq. (1) [10].

$$N = B \cdot (P_v - P_0) \quad (1)$$

where  $N$  is permeate flux (kg/m<sup>2</sup>s),  $B$  is vacuum MD coefficient (kg/m<sup>2</sup>s Pa),  $P_v$  is vapor pressure at membrane surface (Pa), and  $P_0$  is applied vacuum pressure (Pa).

$B$  is a value related to the membrane properties and is defined as VMD coefficient. It can be calculated using Eq. (2) [10].  $P_v$  value is the vapor pressure at the membrane surface that can be calculated using Eq. (3).  $P_v$  value is calculated using the temperature ( $T_m$ ) and concentration ( $C_m$ ) at the membrane surface. It is impossible to directly measure the vapor pressure at the membrane surface, thus, the values are obtained through calculation.

Table 1  
Operating condition in this research at a constant steam raiser temperature of 60°C

Feed flow rate (L/h)	Vacuum pressure (mbar)	Concentration (M)
20	70	1–4
20	90	1–4
40	70	1–4
40	90	1–4

$$B = 1.064 \frac{r\varepsilon}{\delta\tau} \cdot \left( \frac{M}{RT_m} \right)^{1/2} \quad (2)$$

where  $r$  is pore size ( $\mu\text{m}$ ),  $\varepsilon$  is porosity (dimensionless),  $\delta$  is thickness ( $\mu\text{m}$ ),  $\tau$  is membrane tortuosity (dimensionless) of membrane,  $M$  is molecular weight of water ( $\text{g/mol}$ ),  $R$  is ideal gas constant ( $\text{J/mol}\cdot\text{K}$ ), and  $T_m$  is feed temperature at the membrane surface ( $\text{K}$ ).

$$P_v = \frac{\exp\left(\frac{-5.8 \times 10^3}{(T_m/\text{K})} + 1.39 + (-4.86 \times 10^{-2}) \cdot (T_m/\text{K}) + (-1.45 \times 10^{-8}) \cdot (T_m/\text{K}) + 6.55 \log(T_m/\text{K})\right)}{1 + 0.57257 \cdot \left(\frac{C_m/(\text{g/kg})}{1000 - C_m/(\text{g/kg})}\right)} \quad (3)$$

where  $T_m$  is feed temperature on the membrane surface ( $\text{K}$ ) and  $C_m$  is feed concentration on the membrane surface ( $\text{g/kg}$ ).

### 2.2.2. Calculation of temperature and concentration at membrane surface, and permeate flux on the System

To predict the permeate flux of the vacuum MD system, the temperature and concentration at the membrane surface must be known. The reason why there is a difference between the feed temperature and concentration at the bulk phase and at the membrane surface is polarization effect. The vapor pressure can be calculated when the temperature ( $T_m$ ) and concentration ( $C_m$ ) of the feed solution at the membrane surface are known.  $T_m$  and  $C_m$  cannot be directly measured, but they must be found through calculation considering temperature polarization and concentration polarization. Thus,  $T_m$  is calculated using Eqs. (1) and (4) and  $C_m$  is calculated using Eqs. (1) and (5) [10–12].

$$h_w(T_b - T_m) = N \cdot H_v \quad (4)$$

where  $h_w$  is heat transfer coefficient ( $\text{kg}/\text{K}\cdot\text{s}^3$ ) and  $T_b$  is bulk feed temperature ( $\text{K}$ ).

$$\ln \frac{C_m}{C_b} = \frac{N}{k} \quad (5)$$

where  $C_b$  is feed concentration ( $\text{g/kg}$ ) and  $k$  is mass transfer coefficient ( $\text{m/s}$ ).

Eqs. (5)–(8) were used to calculate the concentration polarization. Eq. (5) is then rearranged regarding  $C_m$  [13].

$$k = \frac{ShD}{dh} \quad (6)$$

where  $Sh$  is Sherwood number (dimensionless),  $D$  is diffusion coefficient of solute ( $\text{m}^2/\text{s}$ ), and  $dh$  is hydraulic diameter ( $\text{m}$ ).

$$Sh = 1.86 \cdot (ReSc \cdot (dh/Lm))^{0.33} \quad (7)$$

where  $Re$  is Reynolds number (dimensionless),  $Sc$  is Schmidt number (dimensionless), and  $Lm$  is channel length ( $\text{m}$ ).

$$Re = \frac{dh \cdot u \cdot \rho}{\mu} \quad (8)$$

where  $u$  is flow rate ( $\text{L/s}$ ),  $\rho$  is density ( $\text{kg}/\text{m}^3$ ) and  $\mu$  is viscosity ( $\text{kg}/\text{m}\cdot\text{s}$ ).

Temperature polarization is calculated using Eqs. (4), (9), and (10), and Eq. (4) is then rearranged regarding  $T_m$  [13].

$$h_w = \frac{Nu \cdot k_w}{dh} \quad (9)$$

where  $Nu$  is Nusselt number (dimensionless) and  $k_w$  is thermal conductivity of water ( $\text{J}/\text{s}\cdot\text{m}\cdot\text{K}$ ).

$$Nu = 1.86 \cdot \left( Re \cdot Pr \cdot \frac{dh}{Lm} \right)^{0.33} \quad (10)$$

where  $Pr$  is Prandtl number (dimensionless).

This research used modeling program to calculate the temperature and concentration at the membrane surface by considering the temperature polarization and concentration polarization, and to calculate the permeate flux. Fig. 3 is a representation of the process of calculating the permeate flux with considering the temperature and concentration at the membrane surface. In this process, the first step is that the temperature and flow rate of the vapor generated from the steam raiser was calculated by considering temperature polarization and concentration polarization from the steam raiser. Thereafter, the temperature and concentration at the membrane surface was calculated by solving Eqs. (4) and (5) with the simultaneous equations of two unknowns ( $C_m$ ,  $T_m$ ). Eqs. (4) and (5) were

combined with Eq. (1) and other equations, and these equations can be expressed by functions of  $C_m$  and  $T_m$ . In detail, Eq. (4) was combined with Eqs. (1)–(3) and 10, Eq. (5) was coupled with Eqs. (6)–(8). To solve the simultaneous equations, that is Eqs. (4) and (5), the solve function in MATLAB was used. The feed solution temperature at the feed channel was estimated based on the temperature and flow rate of steam generated from the steam raiser using Eq. (11) [14].

$$T_b = \frac{H_{\text{vap}}}{Q_b C_{\text{pw}}} + T \quad (11)$$

where  $H_{\text{vap}}$  is latent heat of vapor (J/s),  $Q_b$  is flow rate of steam from the previous stage ( $\text{m}^3/\text{s}$ ), and  $C_{\text{pw}}$  is thermal capacity (J/kg·K).

Once this calculation is complete, the concentration and temperature at the membrane surface of the membrane module are calculated. These are calculated using the same step as calculating the temperature and concentration at the membrane surface at the steam raiser. The permeate flux is calculated using the calculated membrane surface temperature and concentration.

### 3. Result and discussion

#### 3.1. Influence of operating parameters

Fig. 4 presents the experimental and modeling results of the permeate flux variation according to operating conditions. The permeate flux value based on operating conditions is given in the Table 2. The extent of the impact on the permeate flux by varied operating was examined by comparing the variation of permeate flux for each condition.

To analyze the impact of vacuum pressure on the permeate flux, an experiment was carried out under different vacuum pressures of 70 and 90 mbar at a feed flow rate of 20 L/h and salinity of 1 M of NaCl. When operation was carried out with a vacuum pressure set to 90 mbar, the permeate flux was approximately 9.30  $\text{kg}/\text{m}^2\text{h}$  and when the operation was carried out with 70 mbar, the permeate flux was about 11.01  $\text{kg}/\text{m}^2\text{h}$ . The permeate flux was increased by 18.4% when the vacuum pressure reduced by 20 mbar at a feed flow rate of 20 L/h.

Meanwhile, the permeate flux increased by approximately 30.4% when the vacuum pressure reduced by 20 mbar at a feed flow rate of 40 L/h. When the vacuum pressure was set at 90 mbar, the permeate flux was

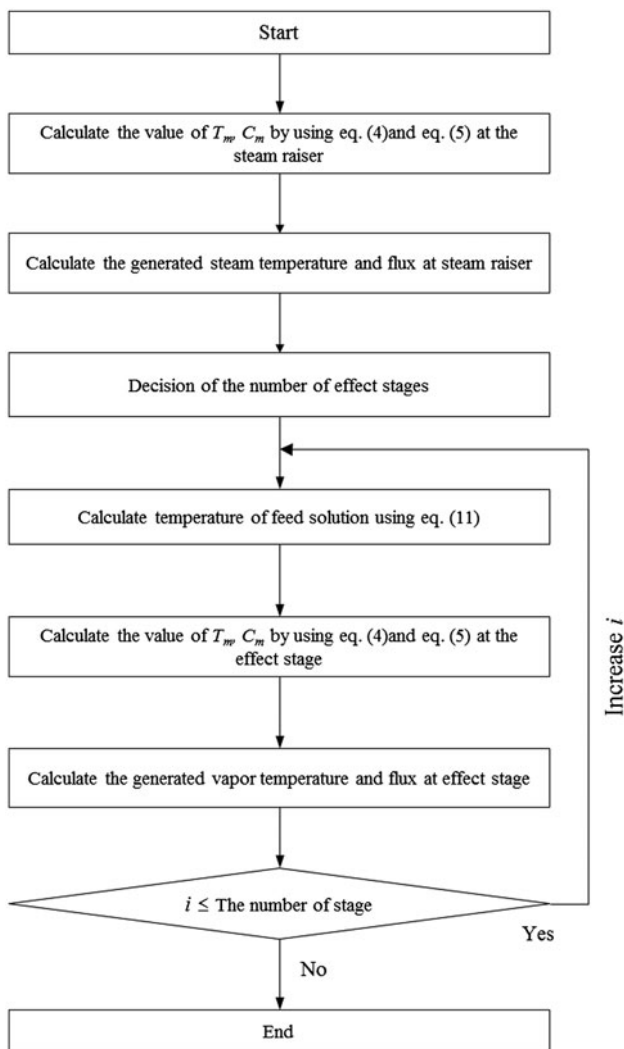


Fig. 3. Algorithm of calculation on V-MEMD permeate flux.

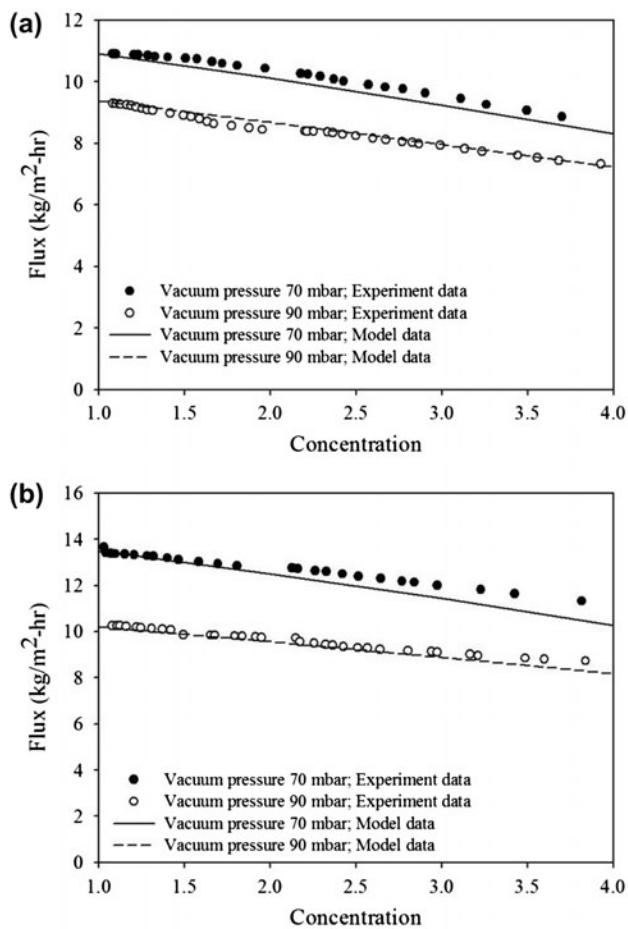


Fig. 4. The variation of flux with different operating conditions at different feed flow rate (a) 20 L/h and (b) 40 L/h.

10.29 kg/m<sup>2</sup>h and when the operation was carried out by lowering the vacuum pressure to 70 mbar with the same flow rate, the permeate flux was 13.50 kg/m<sup>2</sup>h.

Variation on vacuum pressure changes  $P_0$  in Eq. (1), and this changes  $\Delta P$  when calculating the permeate flux. Membrane transfer resistance can be reduced as  $\Delta P$  grows, and as the vacuum pressure becomes lower, it can result in reduced thermal loss.

Hence, a higher permeate flux value was achieved when lower vacuum pressure was applied as shown in the experimental value. The modeling permeate value is in line with the experimental results.

Increasing the feed flow rate, on the other hand, would increase the turbulence and reduced the boundary layer on membrane surface, and it makes increasing the permeate flux. However, when analyzing based on the variation of the permeate flux, it was more impacted by the vacuum pressure than flow rate. Because the variation of permeate flux according to changes in vacuum pressure is greater than feed flow rate.

Increasing the feed salinity from 1 to 4 M resulted in permeate flux reduction ratio of only 15–20% for all experiment conditions. The permeate flux decreased about 20 and 16% when feed concentration increased 1–4 M at feed flow rate 20 and 40 L/h, respectively.

The results showed that a 15–16% reduction ratio of permeate flux was made only when the feed flow rate was increased from 20 to 40 L/h. On the other hand, around 18–20% reduction ratio of permeate flux was observed only when the vacuum pressure was reduced. This shows that a higher feed flow rate was important to maintain a reasonable flux in comparison to vacuum pressure with increased feed salinity. This is because when vacuum pressure decreases, the heat transfer rate decreases and mass transfer rate increases due to mass transfer resistance decrease. Thus, it makes higher permeate flux. And, increased feed flow rate played an important role of increasing turbulence, reducing the boundary layer at the membrane surface, and minimizing the concentration polarization effect.

The permeate flux was approximately 14 kg/m<sup>2</sup>h at 60°C and 4 M NaCl in DCMD[15]. But, in this study, the permeate flux was in 7.30–8.67 kg/m<sup>2</sup>h at same temperature and concentration. The flux difference between DCMD and V-MEMD is attributed to the permeate side condition.

Table 2

The variation of flux with operating condition (unit: kg/m<sup>2</sup> h)

Concentration of feed solution (M)	Set I (70 mbar, 20 L/h)		Set II (90 mbar, 20 L/h)		Set III (70 mbar, 40 L/h)		Set IV (90 mbar, 40 L/h)	
	Experiment flux	Model flux	Experiment flux	Model flux	Experiment flux	Model flux	Experiment flux	Model flux
1	11.01	10.92	9.30	9.31	13.42	13.51	10.29	10.21
2	10.36	10.11	8.42	8.68	12.78	12.50	9.73	9.57
3	9.54	9.25	7.92	7.96	12.00	11.45	9.09	8.88
4	8.75	8.60	7.30	7.26	11.25	11.28	8.67	8.58

### 3.2. Rejection rate

Rejection rate was calculated by TDS, the system achieved a rejection rate that is more than 99.9%, even at high-salinity feed (1–4 M of NaCl) as shown in Table 3. This means that the V-MEMD system can operate even under high salinity condition. The TDS was measured in permeate tank. As shown Fig. 5, Permeate TDS is normally below 100  $\mu\text{m}/\text{cm}$ .

### 3.3. Polarization effect

#### 3.3.1. Concentration polarization

In this study, an analysis of concentration polarization effect with different operating condition was carried out, and a ratio of concentration at membrane surface ( $C_m$ ) over the bulk concentration ( $C_b$ ) was used for calculation of extent of concentration polarization [15]. The ratio of  $C_m/C_b$  is closer to 1 meaning that the polarization occurs less.

The concentration polarization ratio in this system varied in the range of 1.135–1.349 in Table 4. The lowest concentration polarization effect at 1.135 was observed at 90 mbar, 4 M NaCl, and 40 L/h. The highest concentration polarization effect of 1.349 was observed at 90 mbar, 1 M NaCl, and 20 L/h.

Eq. (5) was used to calculate the  $C_m$  value to evaluate the concentration polarization ratio. The  $N$  value increases with lower vacuum pressure and

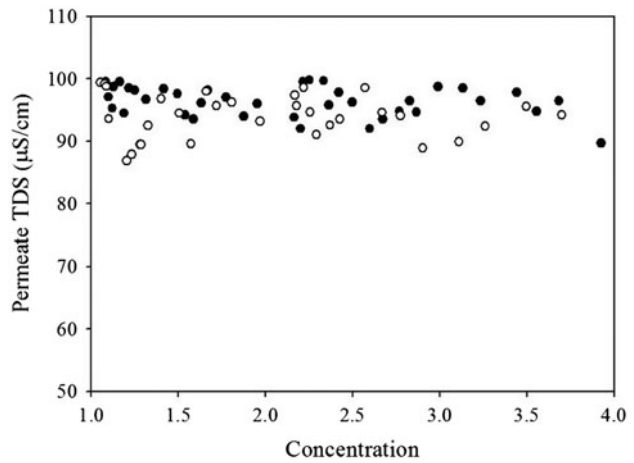


Fig. 5. The variation of permeate TDS with operating condition.

concentration at membrane surface ( $C_m$ ). Thus, a higher concentration polarization effect was presented. At increasing feed flow rate,  $k$  value (mass transfer coefficient) grows and  $C_m$  value decreases, and hence, the extent of concentration polarization reduced.  $k$  value can be obtained using Eqs. (6)–(8).

At increased feed concentration, a lower concentration polarization effect was presented. The reason is because once the feed concentration grows higher, the  $C_m$  value increases, and hence, the  $P_v$  value grows

Table 3  
Salt rejection rate of each condition

Concentration of feed solution (M)	Set I (70 mbar, 20 L/h)	Set II (90 mbar, 20 L/h)	Set III (70 mbar, 40 L/h)	Set IV (90 mbar, 40 L/h)
Rejection rate (%)	99.92	99.88	99.89	99.84

Table 4  
The reduction rate of vapor pressure with operating condition

Operating condition	Concentration of feed solution (M)	$P_v/P_b$	Temperature polarization		Concentration polarization	
			1 – TP	$P_{v,T}(T_m, C_b)/P_b$	CP – 1	$P_{v,C}(T_b, C_m)/P_b$
90 mbar	1	0.667	0.024	0.672	0.215	0.992
20 L/h	4	0.751	0.016	0.771	0.135	0.973
90 mbar	1	0.670	0.024	0.679	0.212	0.992
40 L/h	4	0.753	0.015	0.774	0.133	0.974
70 mbar	1	0.530	0.037	0.554	0.349	0.987
20 L/h	4	0.595	0.028	0.627	0.251	0.950
70 mbar	1	0.536	0.037	0.543	0.343	0.987
40 L/h	4	0.600	0.028	0.631	0.247	0.951

smaller. Consequently, the  $N$  value grows small, the difference between  $C_b$  and  $C_m$  values becomes smaller as shown in Fig. 6.

### 3.3.2. Temperature polarization

Fig. 7 shows the variation of the extent of temperature polarization according to changes in operating conditions. In this study, the effect of temperature polarization is defined by the temperature polarization ratio ( $T_m/T_b$ ) [16]. Hence, a temperature polarization ratio becomes closer to 1, which is interpreted as low effect of temperature polarization.

Overall the temperature polarization ratio for the operating condition in this study has range from 0.963 to 0.985. Reducing the vacuum pressure (90–70 mbar) resulted in higher temperature polarization effect by an increase of 0.013 in ratio. A higher feed salinity (1–4 M of NaCl) lowers the temperature polarization effect by a reduction of 0.008 in ratio. Increasing the feed flow rate (20–40 L/h) resulted in lower temperature polarization effect. At this flow ranges, although the effect on temperature polarization was insignificant, the permeate flux change is relatively high.

### 3.3.3. Analysis of contribution of polarization to permeate flux reduction

In this study, vapor pressure value was used to explain the influence of concentration polarization and temperature polarization on permeate flux. This is because as represented by Eq. (1), vapor pressure is the driving force on the permeate flux. A variation of vapor pressure directly represents variation in the

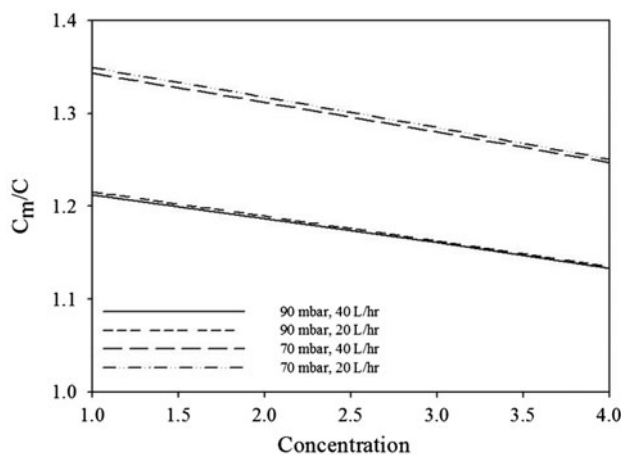


Fig. 6. The variation of extent of concentration polarization with operating condition.

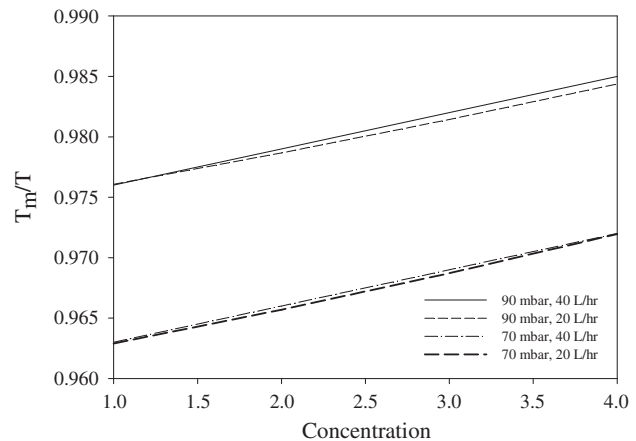


Fig. 7. The variation of extent of temperature polarization with operating condition.

permeate flux. A vapor pressure reduction ratio that is  $P_v/P_b$  ( $P_v$ , vapor pressure at membrane surface and  $P_b$ , the vapor pressure at feed bulk phase) is adopted in this study. The vapor pressure incorporating only temperature polarization ( $P_{v,T}(T_m, C_b)$ ), only concentration polarization ( $P_{v,C}(T_b, C_m)$ ), and both of this ( $P_v(T_m, C_m)$ ;  $P_v$ ) was estimated and compared with  $P_b$ .

Table 4 shows the vapor pressure difference with operating conditions considering temperature and concentration polarization. The value of  $P_{v,C}(T_b, C_m)/P_b$ , that is, the vapor pressure difference considering only concentration polarization was in the range of 0.950–0.992. Since this value was almost close to 1, it can be concluded that the effect of concentration polarization to vapor pressure drop has almost no impact in all experimental condition.

In contrast,  $P_{v,T}(T_m, C_b)/P_b$ , that is, the vapor pressure difference considering only temperature polarization was at a much lower range of 0.543–0.774. However, the temperature polarization effect for all experimental condition was actually at a high range of 0.963–0.985 as described in Section 3.3.2. This is because, for the calculation of membrane surface vapor pressure, membrane surface feed temperature is exponentially measured as represented by Eq. (3). This means that even a small drop of 1–2°C of feed temperature exponentially reduce the value of vapor pressure at membrane surface. For instance, at a minimal temperature polarization ratio of 0.985, vapor pressure ratio was reduced to 0.774. In this case, increased feed flow rate appears to be important to maintain a higher vapor pressure ratio.

As shown Fig. 8, extent of concentration polarization is larger than temperature polarization. But  $P_{v,T}(T_m, C_b)/P_b$  is much bigger than  $P_{v,C}(T_b, C_m)/P_b$  and is

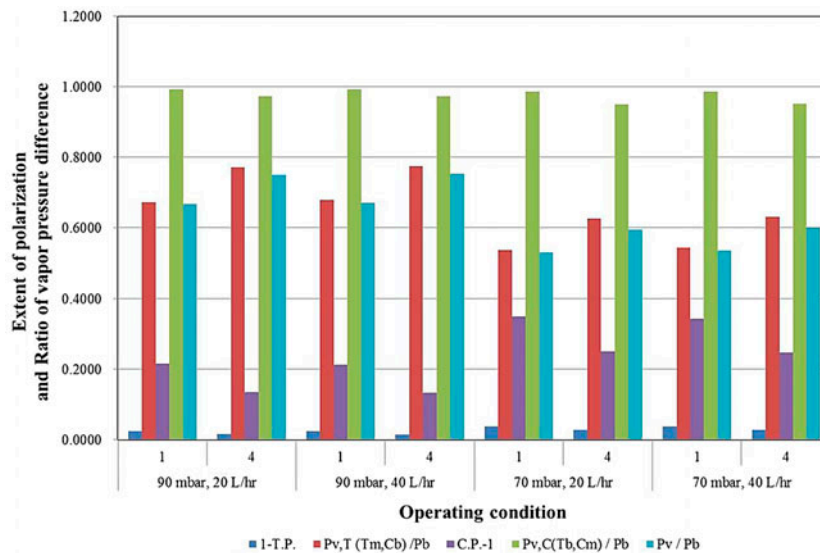


Fig. 8. Extent of polarization and reduction ratio of vapor pressure with different operating condition.

similar with  $P_v/P_b$ . It means that temperature polarization is more dominant for vapor pressure reduction than concentration polarization.

#### 4. Conclusion

This study was conducted to examine the impact of vacuum pressure, feed flow rate, and the feed concentration on the permeate flux in a vacuum MD system. Further, the impact of temperature polarization and concentration polarization was also investigated. The results are as follows:

(1) The 30.4% increase of permeate flux was achieved with a lower vacuum pressure (70 mbar). The 21.8% increase of permeate flux was achieved at higher feed flow rate (40 L/h). Both vacuum pressure and feed flow rate influenced permeate flux positively, with vacuum pressure having a higher impact at lower feed salinity and feed flow rate at higher feed salinity.

(2) The increase of feed water salinity from 1 to 4 M NaCl reduced the permeate flux by 16–20%. Further, the rejection rate was over 99.8%, which means the vacuum MD process is not sensitive to the salinity of the feed solution. This indicates that the V-MEMD process can be used for the treatment of high-salinity water.

(3) A dominant reduction ratio of vapor pressure was observed even at a low ratio of temperature polarization. The vapor pressure little affected by concentration polarization. As the vapor pressure is highly sensitive to temperature change and is the

driving force for the system, it is important to maintain a minimal temperature change. For this purpose, a higher feed flow rate was necessary.

(4) Overall, although vacuum pressure increases the permeate flux by about 30%, it significantly reduces the vapor pressure ratio to 0.6. On the other hand, feed flow rate increased the permeate flux by 2% while maintaining the vapor pressure difference ratio at 0.7. For this system, at a feed temperature of 60°C, it appears to be sustainable to maintain a higher range of feed flow rate as well as vacuum pressure resulting in a sustainable permeate flux of 8.7–10.3 kg/m<sup>2</sup>h at high feed salinity.

#### Acknowledgments

This subject is supported by Ministry of Oceans and Fisheries (MOF) as “Development of Osmotic Energy Driven Shipboard Desalination System” and Korea Institute of Construction Technology (KICT) as “Smart Water-Grid project (2014-0023)”.

#### References

- [1] M. Safavi, T. Mohammadi, High-salinity water desalination using VMD, *Chem. Eng. J.* 149 (2009) 191–195.
- [2] M. Tomaszewska, Membrane distillation—Examples of applications in technology and environmental protection, *Pol. J. Environ. Stud.* 9(1) (2000) 27–36.
- [3] A. Alkhudhiri, N. Darwish, N. Hilal, Membrane distillation: A comprehensive review, *Desalination* 287 (2012) 2–18.

- [4] R.B. Saffarini, E.K. Summers, H.A. Arafat, V.J.H. Lienhard, Technical evaluation of stand-alone solar powered membrane distillation systems, *Desalination* 286 (2012) 332–341.
- [5] T. Mohammadi, M.A. Safavi, Application of Taguchi method in optimization of desalination by vacuum membrane distillation, *Desalination* 249 (2009) 83–89.
- [6] J. Phattaranawik, R. Jiratananon, A.G. Fane, Heat transport and membrane distillation coefficients in direct contact membrane distillation, *J. Membr. Sci.* 212 (2003) 177–193.
- [7] M.S. El-Bourawi, Z. Dinga, R. Ma, M. Khayet, A framework for better understanding membrane distillation separation process, *J. Membr. Sci.* 285 (2008) 4–29.
- [8] K.W. Lawson, D.R. Lloyd, Membrane distillation. I. Module design and performance evaluation using vacuum membrane distillation, *J. Membr. Sci.* 120 (1996) 111–121.
- [9] K. Zhao, W. Heinzl, M. Wenzel, S. Büttner, F. Bollen, G. Lang, S. Heinzl, N. Sarda, Experimental study of the memsys vacuum-multi-effect-membrane-distillation (V-MEMD) module, *Desalination* 323 (2013) 150–160.
- [10] J.I. Mengual, M. Khayet, M.P. Godino, Heat and mass transfer in vacuum membrane distillation, *Int. J. Heat Mass Transfer* 47 (2004) 865–875.
- [11] M.H. Sharqawy, J.H. Lienhard, S.M. Zubair, Thermophysical properties of seawater: A review of existing correlations and data, *Desalin. Water Treat.* 16 (2010) 354–380.
- [12] M. Khayet, Membranes and theoretical modeling of membrane distillation: A review, *Adv. Colloid Interface Sci.* 164 (2011) 56–88.
- [13] L. Martínez-Díez, M.I. Vázquez-González, Temperature and concentration polarization in membrane distillation of aqueous salt solutions, *J. Membr. Sci.* 156 (1999) 265–273.
- [14] F. Banat, F.A. Al-Rub, K. Bani-Melhem, Desalination by vacuum membrane distillation: Sensitivity analysis, *Sep. Purif. Technol.* 33 (2003) 75–87.
- [15] F. Edwie, T.S. Chung, Development of hollow fiber membrane for water and salt recovery from highly concentrated brine via direct contact membrane distillation and crystallization, *J. Membr. Sci.* 421 (2012) 111–123.
- [16] J. Mericq, S. Laborie, C. Cabassud, Vacuum membrane distillation of seawater reverse osmosis brines, *Water Res.* 44 (2010) 5260–5273.